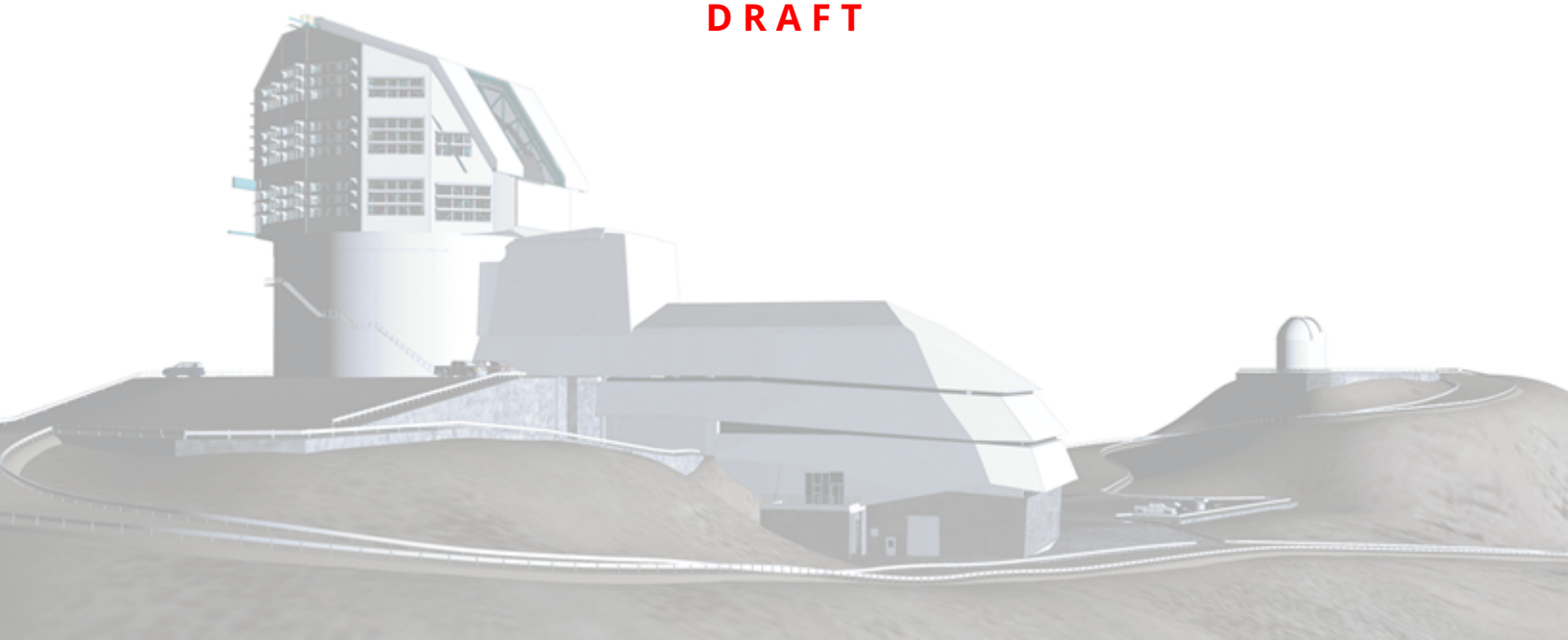

Vera C. Rubin Observatory
Systems Engineering

An Interim Report on the ComCam On-Sky Campaign

Many authors

SITCOMTN-149

Latest Revision: 2024-11-25

DRAFT

Abstract

A summary of what we have learned from the initial period of ComCam observing

Change Record

Version	Date	Description	Owner name
1	YYYY-MM-DD	Unreleased.	Robert Lupton

Document source location: `https://github.com/lsst-sitcom/sitcomtn-149`

Contents

An Interim Report on the ComCam On-Sky Campaign

1 Introduction

The Vera C. Rubin Observatory on-sky commissioning campaign using the Commissioning Camera (ComCam) began on 24 October 2024 and is forecasted to continue through mid-December 2024. This interim report provides a concise summary of our understanding of the integrated system performance based tests and analyses conducted during the first weeks of the ComCam on-sky campaign. The emphasis is distilling and communicating what we have learned about the system. The report is organized into sections to describe major activities during the campaign, as well as multiple aspects of the demonstrated system and science performance.

Warning: Preliminary Results

All of the results presented here are to be understood as work in progress using engineering data. It is expected at this stage, in the middle of on-sky commissioning, that much of the discussion will concern open questions, issues, and anomalies that are actively being worked by the team. Additional documentation will be provided as our understanding of the demonstrated performance of the as-built system progresses.

1.1 Charge

We identify the following high-level goals for the interim report:

- **Rehearse workflows for collaboratively developing documentation** to describe our current understanding of the integrated system performance, e.g., to support the development of planned Construction Papers and release documentation to support the Early Science Program [RTN-011]. This report represents an opportunity to collectively exercise the practical aspects of developing documentation in compliance with the policies and guidelines for information sharing during commissioning [SITCOMTN-076].
- **Synthesize the new knowledge** gained from the ComCam on-sky commissioning cam-

paign to inform the optimization of activities between the conclusion of the ComCam campaign and the start of the on-sky campaign with the LSST Camera (LSSTCam).

- **Inform the Rubin Science Community** on the progress of the on-sky commissioning campaign using ComCam.

Other planned systems engineering activities will specifically address system-level verification ([LSE-29] and [LSE-30]) using tests and analysis from the ComCam campaign. While the analyses in this report will likely overlap with the generation of verification artifacts for systems engineering, and system-level requirement specifications will serve as key performance benchmarks for interpreting the progress to date, formal acceptance testing is not an explicit goal of this report.

The groups within the Rubin Observatory project working on each of the activities and performance analyses are charged with contributing to the relevant sections of the report. The anticipated level of detail for the sections ranges from a paragraph up to a page or two of text, depending on the current state of understanding, with **quantitative performance** expressed as summary statistics, tables, and/or figures. The objective for this document is to **summarize the state of knowledge of the system**, rather than how we got there or "lessons learned". The sections refer to additional supporting documentation, e.g., analysis notebooks, other technotes with further detail, as needed. Given the timelines for commissioning various aspects of the system, it is natural that some sections will have more detail than others.

The anticipated milestones for developing this interim report are as follows:

- 18 Nov 2024: Define charge
- 4 Dec 2024: First drafts of report sections made available for internal review
- 11 Dec 2024: Revised drafts of report sections made available for internal review; editing for consistency and coherency throughout the report
- 18 Dec 2024: Initial version of report is released

Warning: On-sky Pixel Image Embargo

All pixel images and representations of pixel images of any size field of view, including individual visit images, coadd images, and difference images based on ComCam commissioning on-sky observations must be kept internal to the Rubin Observatory Project team, and in particular, cannot be included in this report. Embargoed pixel images can only be referenced as authenticated links. See [SITCOMTN-076] for details.

2 System Performance Analysis

3 Active Optics System Commissioning

4 Image Quality

5 Data Production

6 Calibration Data

7 Science Pipelines Commissioning Observations

8 Throughput for Focused Light

9 Delivered Image Quality and PSF

10 Instrument Signature Removal

The quality of the instrument signal removal (ISR) has improved during commissioning, as we create and deploy updated calibration products that better represent the LSSTComCam system. The following discussion summarizes our current understanding of a variety of features,

both expected and newly seen on LSSTComCam, and presents our expected prognosis of the behavior of the full LSSTCam.

10.1 Phosphorescence

There are regions on some of the detectors (most visible in R22_S01, detector=1) which show bright emission, particularly at bluer wavelengths, as shown in Figure 1. This is believed to be caused by a thin layer of remnant photo-resist from the manufacturing process that remained on the detector surface, and is now permanent due to the subsequent addition of the anti-reflective coating. In addition to the large areas, there are also discrete point-source-like or cosmic-ray-like defects caused by accumulations of this material. Adding to the difficulty of mitigating these defects is that this photo-resist is known to be phosphorescent, explaining why these regions are more noticeable in the bluer filters.

The initial studies of this show that these features can continue to emit light up to several minutes after they've been illuminated. Due to the long duration of these features, we decided to place manual defect masks over the worst regions. The first of these manual masks takes up about 3.5% of that detector, smaller than but consistent with estimates that this would create a pixel loss of approximately one amplifier.

The ITL detectors in LSSTCam are believed to have been cleaned better, so this should be less of an issue on the full camera.

10.2 Vampire pixels

There are defects on LSSTComCam that have been classified as "vampire" pixels, as they appear as a bright defect with a (generally) axisymmetric region surrounding the bright core, as if the defect is draining charge from its neighbors. The naming is at least broadly correct, as integrating to large radii shows that these regions do appear to conserve charge. There is an intensity dependence that makes these vampire pixels different than standard hot pixels, as these pixels do not show up on dark frames, only on flats and science exposures, where the detector surface is illuminated. After the initial discovery of the bright obvious vampires, we added new masking code that identifies the bright cores that are above 2.0 on the combined flat (pixels that are greater than 200% of the median flat level), and adds circular masks to the defect list. This appears to find the most problematic examples, but as we have improved

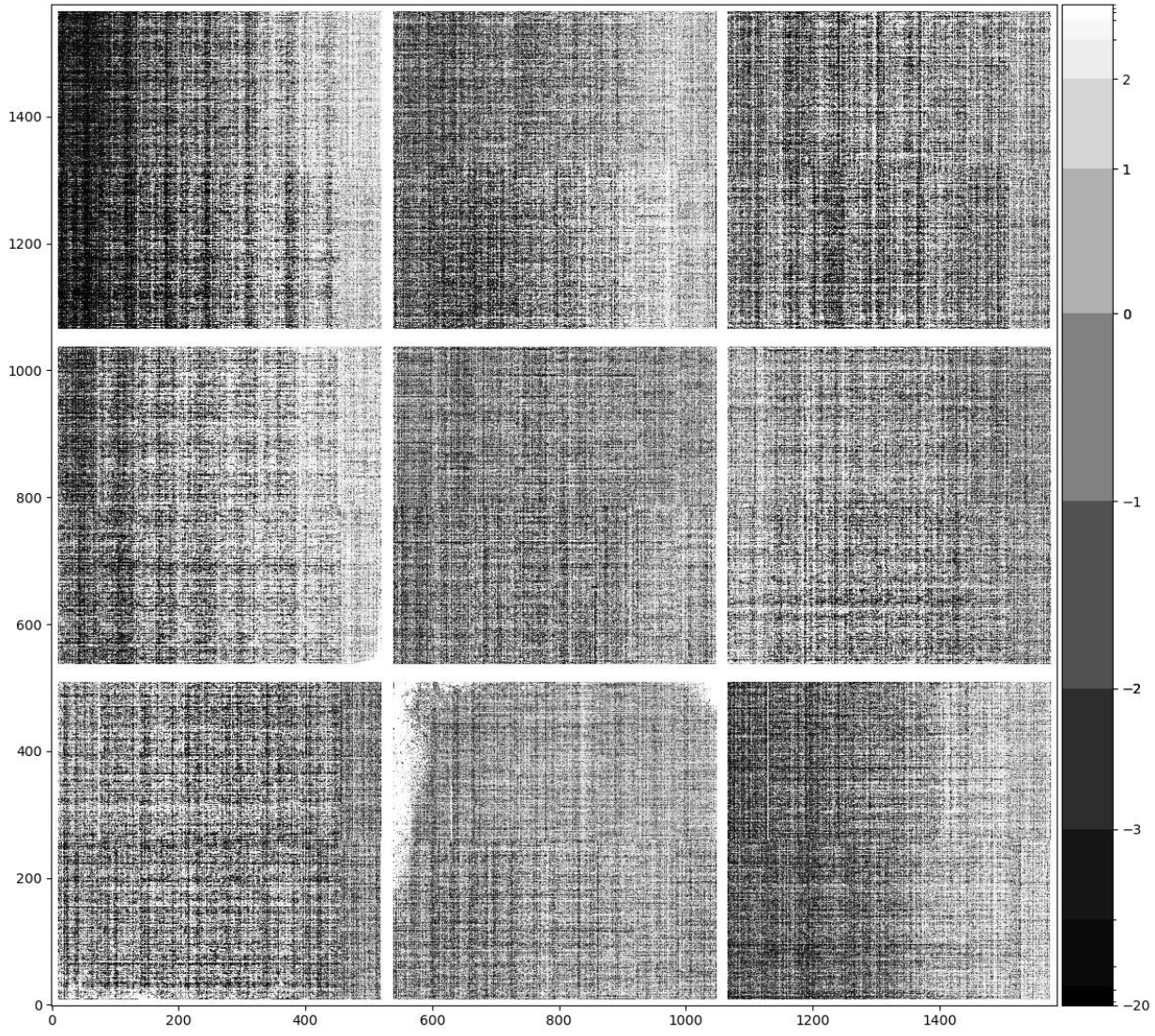

FIGURE 1: The phosphorescence seen in R22_S01, shown here in a dark exposure taken after a series of twilight flats (exposure=2024112000065). This material absorbs light at bluer wavelengths and re-emits that energy over a wide range of wavelengths.

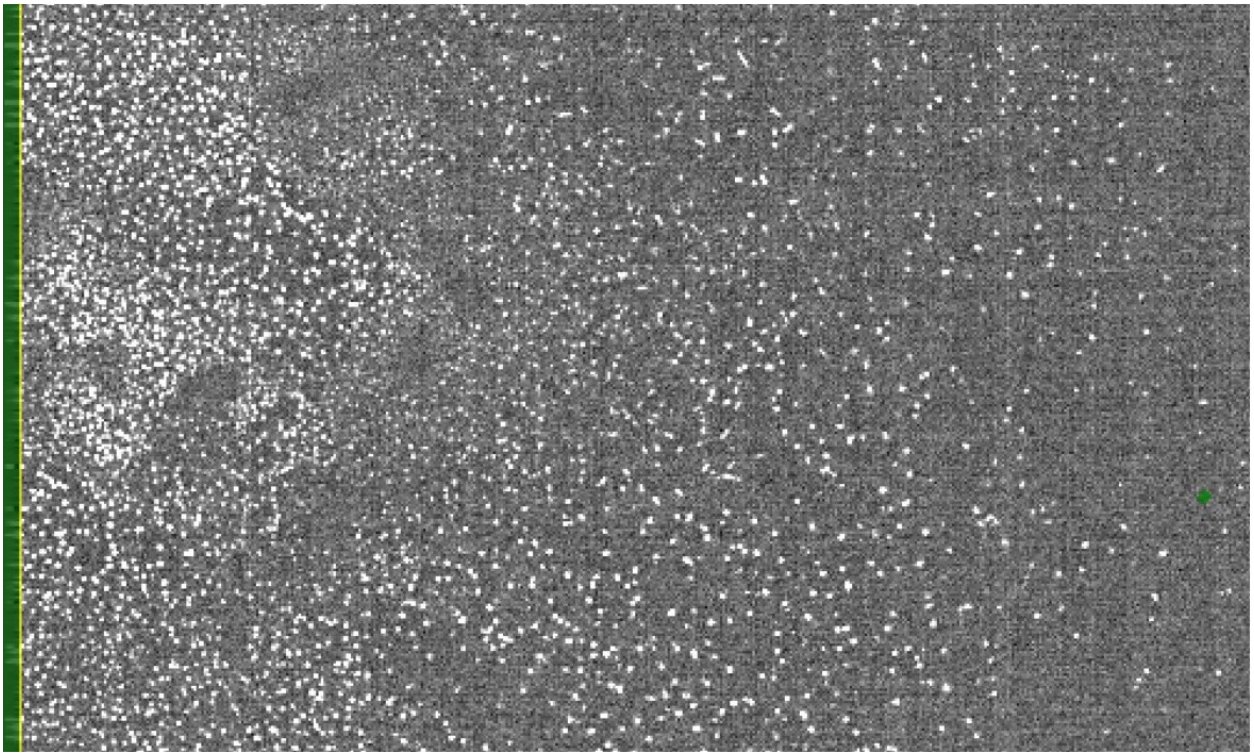

FIGURE 2: A full-resolution view of the edge of R22_S01. The features shown in this image are point-like sources caused by the trapped phosphorescence photo-resist.

flat quality during commissioning, we are finding that there is a sub-population that are not as severe, but likely have a similar physical mechanism. This population is still bright on the flat, with peaks around 1.2 (20% elevated relative to the flat), and may need to be masked as well. From an initial study in the lab, it appears that all ITL detectors on LSSTCam have a few of these kinds of defects, with two detectors approaching similar contamination levels as R22_S10 on LSSTComCam.

10.3 Saturated star effects

Although we expected to find saturated star trails coming from bright sources, the observed behavior of these trails is unique. Saturation spikes on most cameras appear as streaks extending from the core of the bright source along the direction of the parallel transfers, and truncate as the charge bleeds run out of charge (and can no longer overcome the potentials defining the pixel). The trails seem with LSSTComCam, however, extend the entire height of the detectors, crossing the midline break. These trails are also not at the expected high state, with the centers of these trails having flux levels lower than the average sky levels, creating dark trails. On the worst saturated objects, there is also evidence of charge pile-up near the serial readout, which can then create fan-like bright features at the edge of the detector. Those bright features can also then crosstalk onto other amplifiers.

The underlying physics is not well understood, and further study will be needed to see if we can correct these trails outside of the regions of charge buildup. Until we have a correction, we plan to begin masking both the trail and the fan-spread near the serial register.

Although we haven't seen identical features on LATISS, the presence of these odd trails on all LSSTComCam detectors suggests that this is a property of the ITL devices, and so will likely be seen on LSSTCam as well.

10.4 Gain ratios

LSSTComCam has been the first large-scale application of the updated "IsrTaskLSST" task, which uses a model of how the various signals combine to form the raw images to inform how we correct those signals during the ISR process. One improvement of this new task is that we now apply per-amplifier gains before flat correction, removing the gain component that was previously included in the flat correction. This results in the flat containing mainly

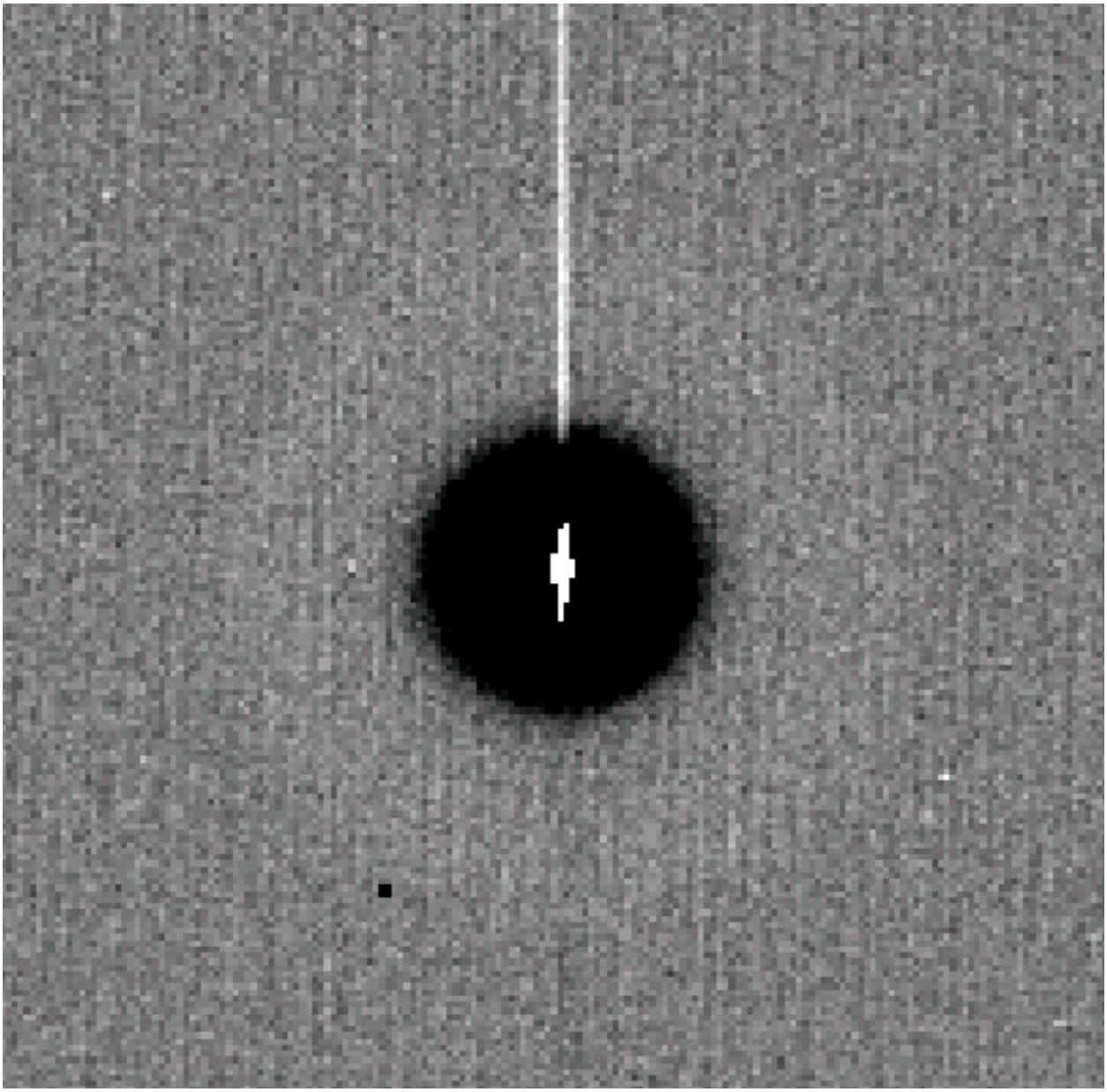

FIGURE 3: A close up of one of the largest vampire pixels. The bright core and region of depletion are clearly visible. Currently we only mask the core and depleted region, but will be extending this to mask the persistence-like trail that this feature leaves in the next few weeks.

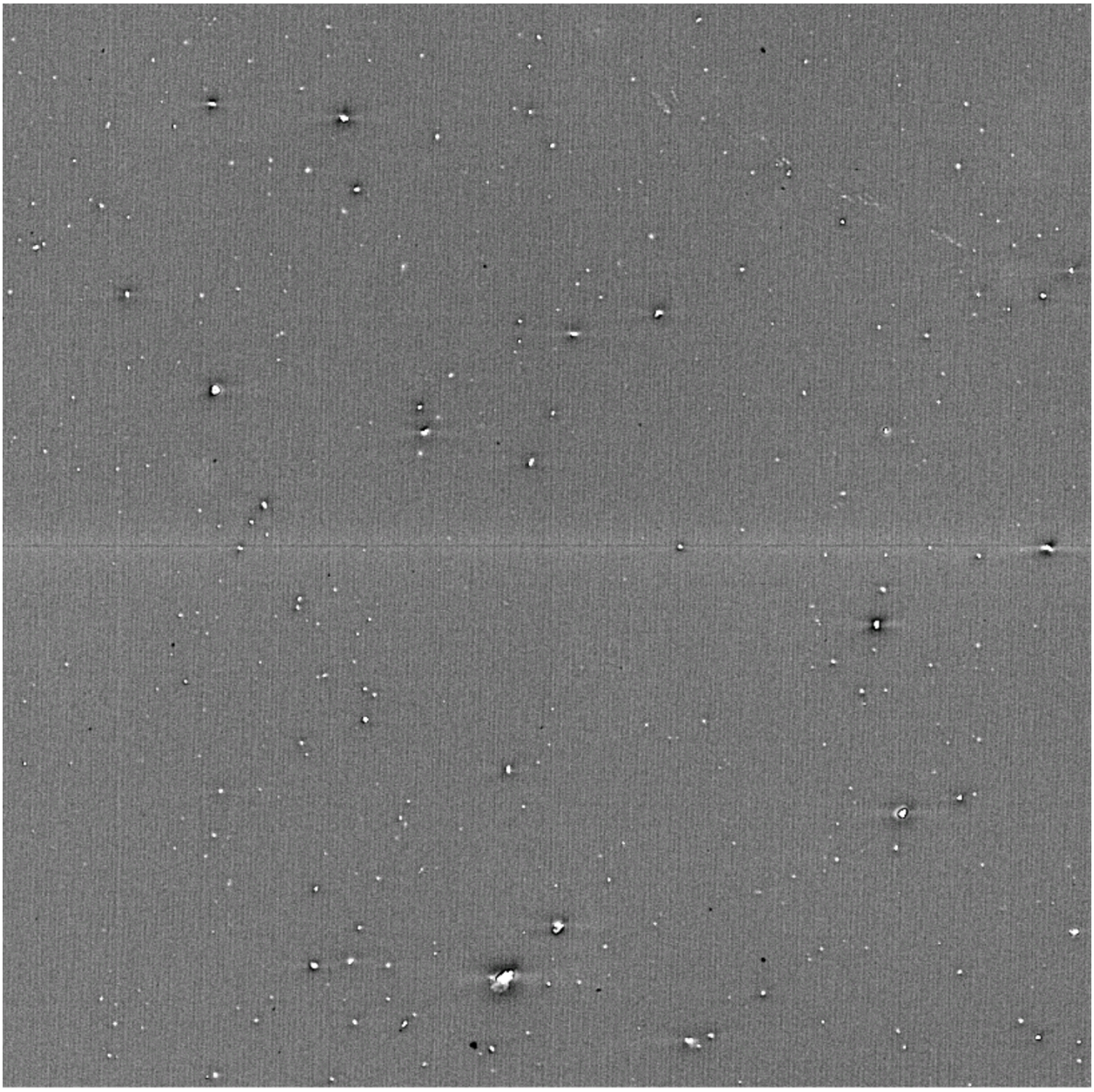

FIGURE 4: A view of detector R22_S10 in y-band, which has a large number of less significant vampire pixels.

QE and illumination patterns, which is much "flatter" than flats that also include gain terms (which offset the amplifiers relative to each other).

If we have properly diagonalized the flats and the gains, we would expect that applying the gain correction would create images with consistent sky levels across different amplifiers. However, when we look at images taken on-sky, our initial gain values result in some amplifiers being significantly different than their neighbors. The gains that we use are derived from the photon transfer curve (PTC), which uses flat pairs at different flux levels to monitor the properties of the noise. We have two of these sequences taken in the lab, and they disagree at the few percent level. This is similar in scale to the errors necessary to explain the on-sky differences. Further complicating this issue, the offsets seen in twilight data (used for flats) and that seen during the night also seem to differ. These differences so far have not been found to correlate with any device temperature, time, or voltage values. The gain correction fix appears to be stable, as we've only needed to generate and apply it once.

10.5 Crosstalk

We are currently using crosstalk values that were constructed by averaging the lab-based ITL measurements taken on LSSTCam. These are working better than expected, with residuals post correction being only a few electrons peak to peak. We plan to do a more complete crosstalk study using on-sky data, but the current results suggest that these lab measurements are sufficient for LSSTComCam, and expect the same to be true for LSSTCam.

10.6 Twilight flats

There is no flat screen currently available for the main telescope, and so we have constructed twilight flats for all bands using exposures taken to have median counts between 15000-20000 ADU. We have some dithering in the inputs, which have allowed us to reduce the impact of stars that print through into the flat. This reduction of non-sky signals is imperfect, and the current i-band flat shows a satellite trail as a result We are working to replace this flat using newly taken data.

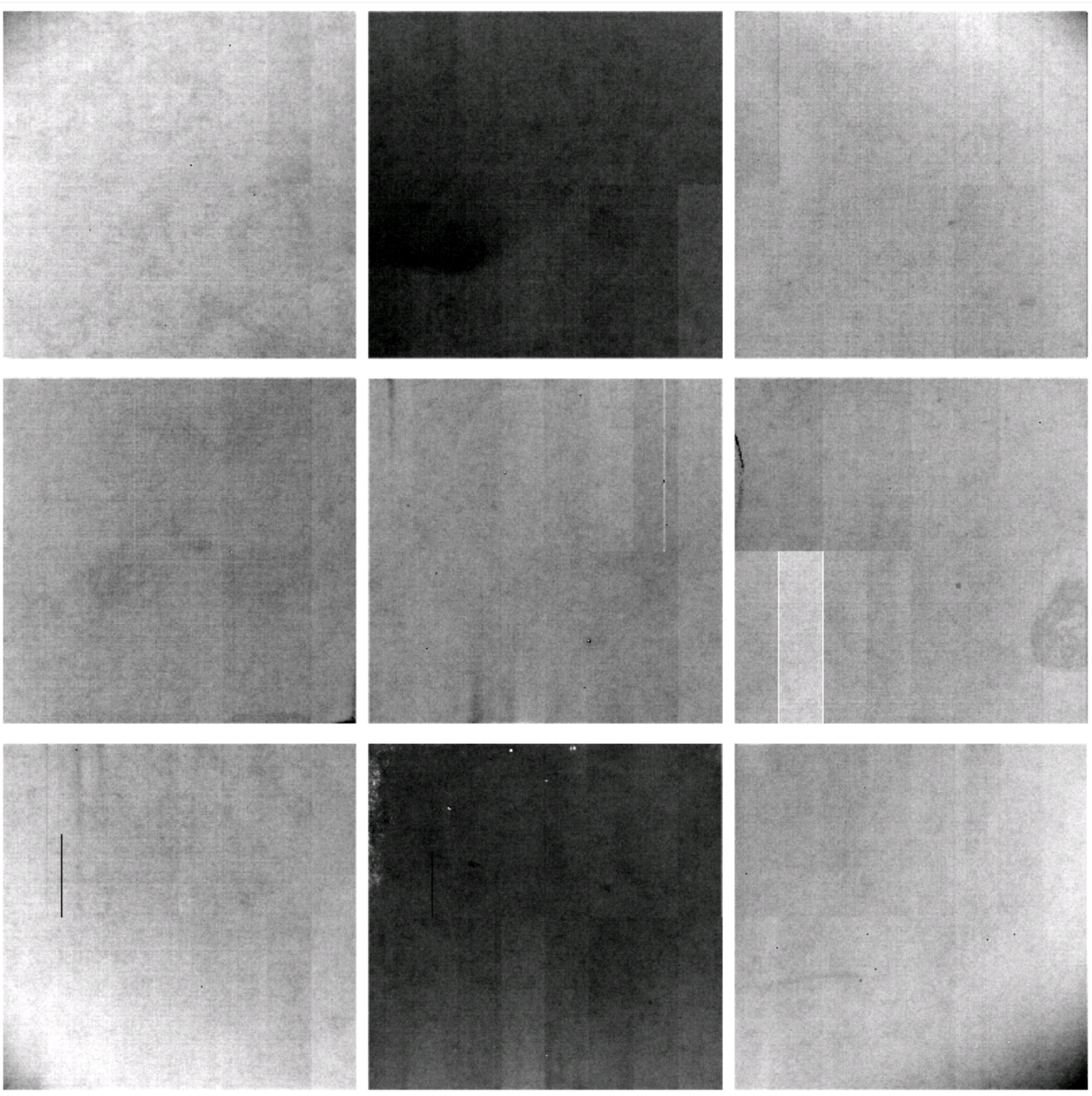

FIGURE 5: The ratio of the twilight-flat divided by a flat constructed from 94 r-band science frames. The scaling ranges from 0.9905 to 1.007. The visibility of amplifiers is caused by the unknown gain errors. The bottom right corner amplifier (C07) on R22_S21 is one of the indicator amplifiers, as it diverges from its neighbors. Although the C00-C03 amplifiers in R22_S12 also show significant offsets, these amplifiers also have an unrelated CTI issue, making them less reliable indicators.

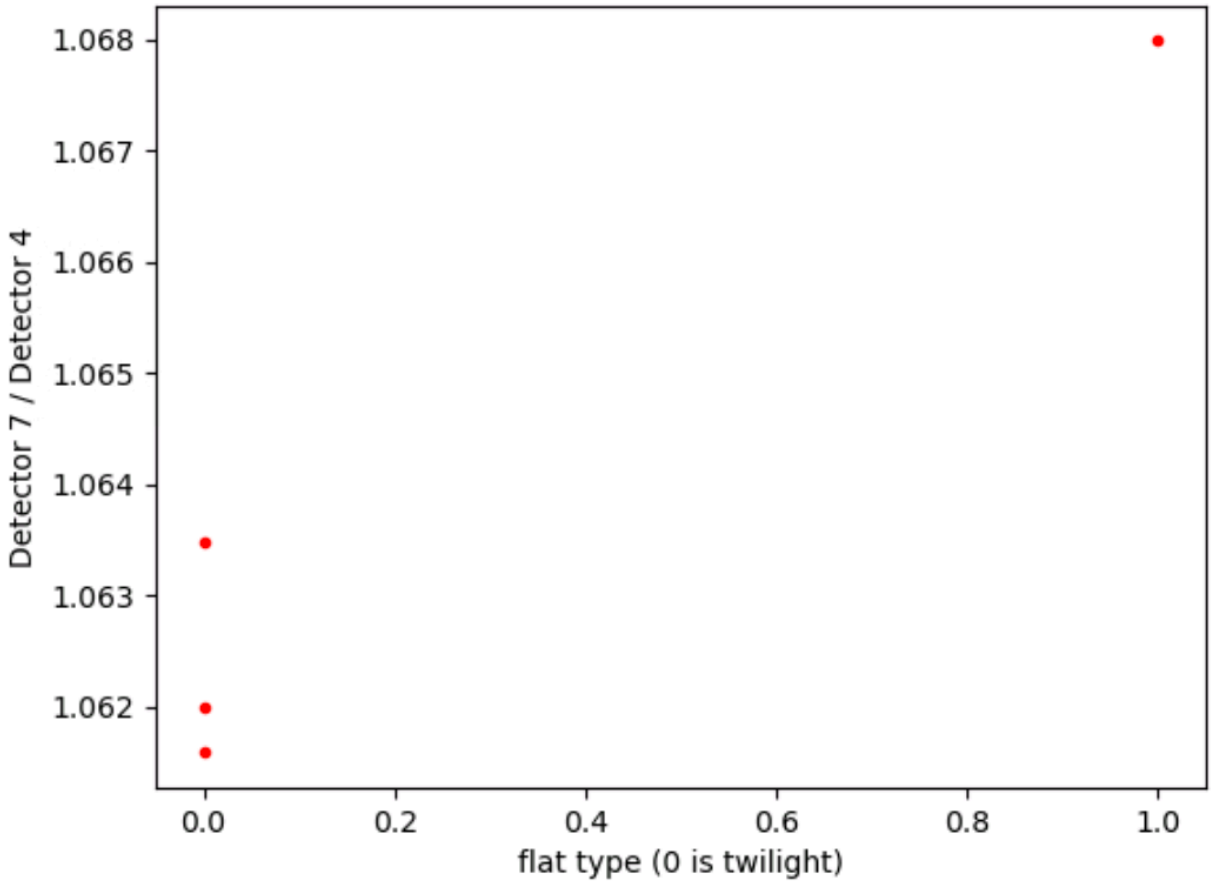

FIGURE 6: A comparison of the gain ratio between amplifiers in R22_S12. C07 is chosen as the indicator amplifier, and C04 is the reference. We have three twilight flat measurements taken at different rotator angles, and one from the 94 input sky flat.

10.7 Operations

The Telescope and Auxiliary Instrumentation Calibration Acceptance Board (TAXICAB) has been meeting previously to discuss LATISS calibrations, and has been helping manage calibrations for LSSTComCam. This process has not prevented problematic calibrations from being deployed (like the i-band flat with the satellite trail), but it has ensured that multiple people have checked some set of results. We are generating calibration verification reports regularly as part of this process (available at `https://s3df.slac.stanford.edu/people/czw/cpv_reports/`), and plan to add new metrics and checks to these as we discover more features of these detectors.

11 Low Surface Brightness

12 Astrometric Calibration

13 Photometric Calibration

14 Survey Performance

15 Sample Production

16 Difference Image Analysis: Transience and Variable Objects

17 Difference Image Analysis: Solar System Objects

17.1 Difference Image Association

So far, difference images have been made only of two fields very far from the ecliptic, where solar system objects are very rare. Known-object association ran, but (correctly) associated no difference image sources to known objects.

17.2 Difference Image Linking

We tested tracklet creation with `make_tracklets`, the first stage of *unknown* asteroid discovery for LSST, on the two available sets of difference images, though asteroids were unlikely to be found in these regions of the sky. The first field included 10 visits with on average 840 sources per visit, while the second had 12 visits with on average 430 sources. These numbers are encouragingly low, indicating that Rubin difference images are fairly clean. For this test case, we set `make_tracklets` to require a minimum of 5 sources per tracklet, but it produced only 9 total tracklets, all with fewer than 5 detections, inconsistent photometry, and relatively high Great Circle residual (GCR)[1]. Manual examination of image cutouts confirmed that the tracklets were entirely composed of spurious sources.

More interesting is the nature of the spurious sources that made up the tracklets. All were associated with bright stars, including diffraction rays, incompletely subtracted scattered light halos, and subtraction residuals near the PSF core. This is very good news, as all of these types of spurious detections can be eliminated through pre-screening of the source catalogs.

Early data suggests that LSST will produce fairly clean difference image source catalogs for the asteroid discovery pipeline and that pre-screening can make them even cleaner. This is important, because simulations indicate the LSST specifications for the minimum discoverable asteroid (six detections, making up three two-point tracklets, within a two-week time span) are on the edge of what is statistically possible without an unacceptable false positive rate. Hence, it is vitally important for the difference image source catalogs to be as clean as possible. There's a lot of work to do, but the early indications have us cautiously optimistic.

18 Single-epoch Image Analysis: Solar System Objects

18.1 Single-epoch Association

Ten images taken in one field on 2024-11-06 and ten each in four fields on 2024-11-23 were close enough to the ecliptic for possible asteroid association. Across the five fields, we associated 828 sources with known asteroids, including 128 unique objects. The 24 objects

[1] Defined only for tracklets with more than two points, the GCR is the RMS residual relative to the best-fit trajectory that follows a Great Circle on the sky at constant angular velocity. Real asteroids, unless they are very near the Earth, produce tracklets with very low intrinsic GCR: hence, elevated GCR usually indicates a spurious tracklet.

associated on 2024-11-06 are shown in Figure 18.1. We compared the sources' astrometry to our ephemerides, as shown in Figure 18.1. We find very low bias: the median unsigned error is 13 mas, indicating that there are no major errors in either timing or astrometry. We also find low variance, with standard deviationsin RA and Dec of 41 and 44 mas respectively, though in an especially bright and therefore low-variance sample of known objects. Evaluating the precision of asteroid association tests the whole software chain, including the astrometry pipeline, ephemerides computation, and image timing. In sum, the total error contributed by these different systems appears to be low enough for high-confidence association of known asteroids.

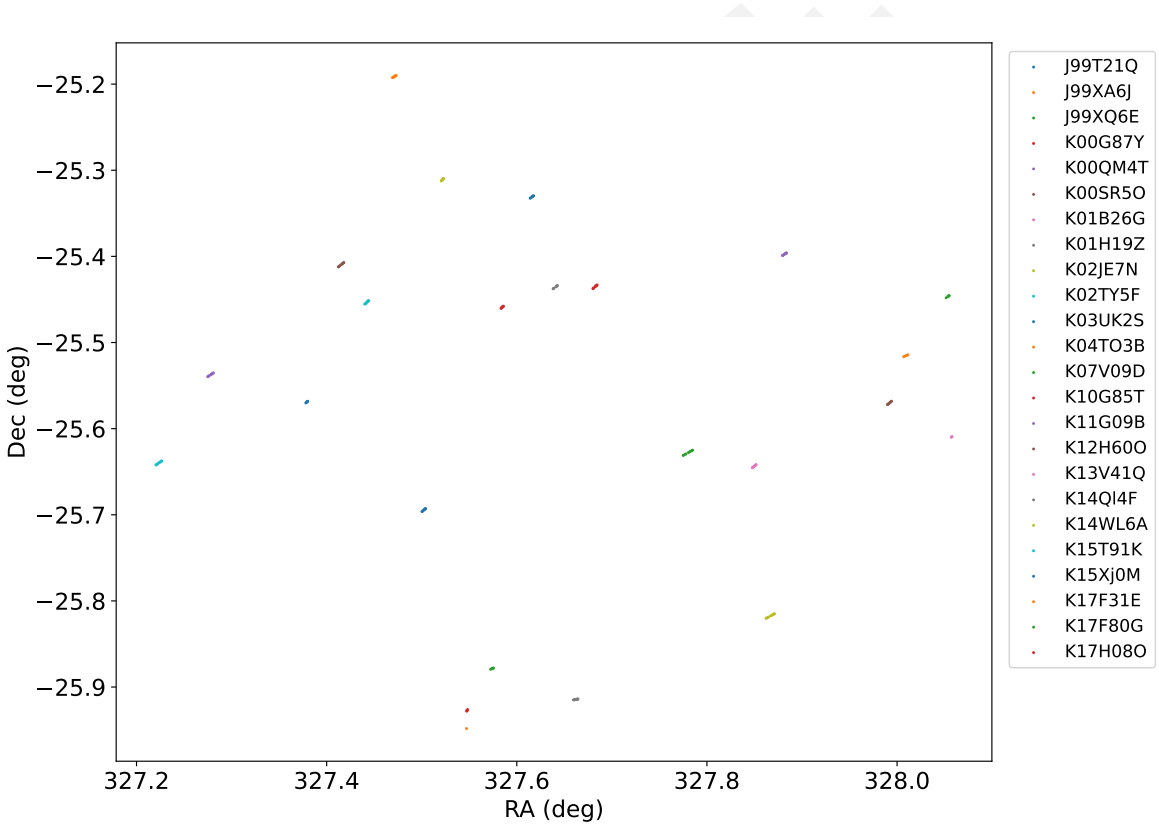

FIGURE 7: Positions of the 24 asteroids associated in images from 2024-11-06.

18.2 Single-epoch Linking

We attempted to link asteroids in single-epoch source catalogs including the fields in section 18.1 relatively near the ecliptic. In contrast to the difference images averaging 430-840 sources per visit, single-epoch images contained 11,000-23,000 sources per visit, mostly stars.

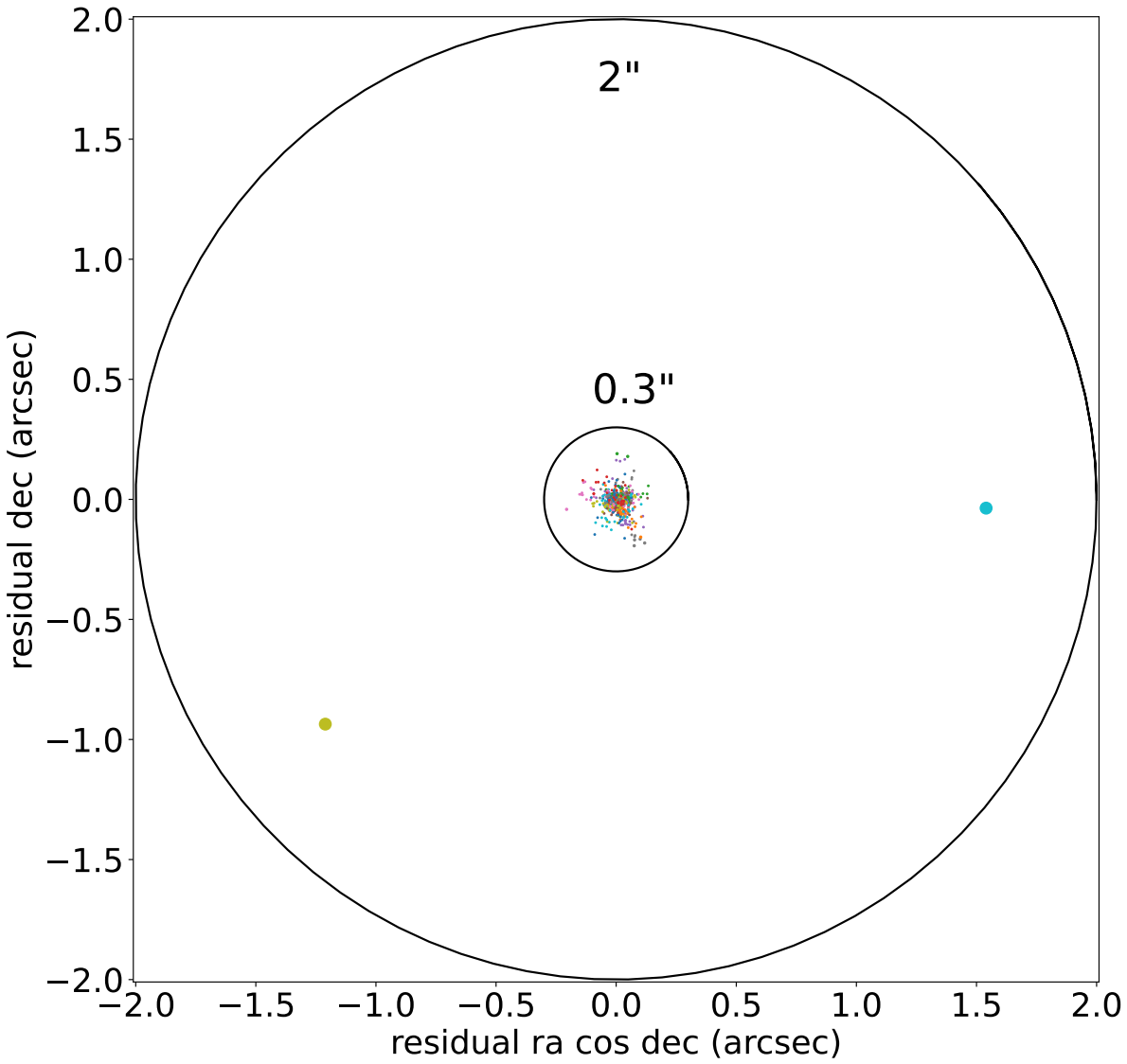

FIGURE 8: Astrometric residuals of the 633 sources associated to 104 asteroids on 2024-11-23. All but two sources have residuals under 0.3 arcseconds, while the two outliers have been identified by visual inspection as mis-associations of undetected asteroids.

The first reasonable test involved ten images taken on November 6. From an average of 16,000 sources per visit, `make_tracklets` found 3,068 tracklets with at least five points. While most of these were unquestionably spurious, nine of them were ten-point tracklets (i.e. detected in *every one* of the ten visits), showed excellent photometric consistency, and relatively low GCR: very likely real asteroids.

We selected the ten-point tracklet with the very lowest GCR (0.046 arcsec) and checked it against known asteroid ephemerides, obtaining a match to the main belt asteroid **(193300) 2000 SO275**, a 20th magnitude object with a very well-constrained orbit. **(193300) 2000 SO275** was the *very first asteroid confirmed to have been detected with the Simonyi Survey Telescope.* We evaluated LSST's astrometric precision by comparing these detections to predicted positions from JPL. The RMS astrometric offset was found to be 29 milli-arcseconds (mas), with a systematic bias (the median observed-calculated residual) of only 14 mas in RA and 3 mas in Dec. These errors are statistically consistent with zero, as expected. We also probed for timing errors, which would produce a positional offset in the direction of motion. Dividing the along-track component of the astrometric offsets by the measured angular velocity, we found a median time offset of 0.3 seconds — consistent with zero at the 0.5σ level.

All of the other ten-point tracklets were found to correspond to known asteroids, as did 12 additional tracklets with 7–9 points, consistent photometry, and relatively low GCR. In total, 21 real asteroids were found by `make_tracklets` in this single field, demonstrating its ability to discover asteroids in LSST catalogs.

19 Galaxy Photometry

20 Weak Lensing Shear

21 Crowded Stellar Fields

22 Image Inspection

A References

[SITCOMTN-076], Bechtol, K., on behalf of the Rubin Observatory Project Science Team, S.R., 2024, Information Sharing during Commissioning, URL https://sitcomtn-076.lsst.io/, Vera C. Rubin Observatory Commissioning Technical Note SITCOMTN-076

[LSE-29], Claver, C.F., The LSST Systems Engineering Integrated Project Team, 2017, LSST System Requirements (LSR), URL https://ls.st/LSE-29, Vera C. Rubin Observatory LSE-29

[LSE-30], Claver, C.F., The LSST Systems Engineering Integrated Project Team, 2018, Observatory System Specifications (OSS), URL https://ls.st/LSE-30, Vera C. Rubin Observatory LSE-30

[RTN-011], Guy, L.P., Bechtol, K., Bellm, E., et al., 2024, Rubin Observatory Plans for an Early Science Program, URL https://rtn-011.lsst.io/, Vera C. Rubin Observatory Technical Note RTN-011

B Acronyms

Acronym	Description
ADU	Analogue-to-Digital Unit
ISR	Instrument Signal Removal
ITL	Imaging Technology Laboratory (UA)
JPL	Jet Propulsion Laboratory (DE ephemerides)
LATISS	LSST Atmospheric Transmission Imager and Slitless Spectrograph
LSST	Legacy Survey of Space and Time (formerly Large Synoptic Survey Telescope)
PSF	Point Spread Function
QE	quantum efficiency
RA	Risk Assessment
RMS	Root-Mean-Square
RTN	Rubin Technical Note
SE	System Engineering